Fuel 220 (2018) 296–302

Contents lists available at ScienceDirect

Fuel

journal homepage: www.elsevier.com/locate/fuel

Full Length Article

A new prediction method for the viscosity of the molten coal slag. Part 1: The effect of particle morphology on the suspension viscosity

Jie Zhou[a,b], Zhongjie Shen[a,b], Qinfeng Liang[a,b,c], Jianliang Xu[a,b], Haifeng Liu[a,b,*]

[a] Key Laboratory of Coal Gasification and Energy Chemical Engineering of Ministry of Education, East China University of Science and Technology, P.O. Box 272, Shanghai 200237, PR China

[b] Shanghai Engineering Research Center of Coal Gasification, East China University of Science and Technology, P.O. Box 272, Shanghai 200237, PR China

[c] State Key Laboratory of Coal Conversion, Institute of Coal Chemistry, Chinese Academy of Sciences, Taiyuan, PR China

ARTICLE INFO

Keywords:
Suspension viscosity
Particle size
Particle shape
Particle aspect ratio
Viscosity model

ABSTRACT

Viscosity is the key factor affecting the flowability of molten coal slag in the entrained flow gasifier. The volume fraction and morphology of solid phase in slag are important factors affecting the slag viscosity. In this study, the malt syrup and the particles with different sizes and morphologies were chosen as the simulation medium to study the effect of particle morphology on the suspension viscosity. The influences of size, shape and aspect ratio of solid particles on the suspension viscosity were considered. It was concluded that the suspension viscosity increased with the decrease of the particle size. The suspension viscosity increased with the increase of the aspect ratio of the particles. This phenomenon was more obvious under the high volume fraction of solid phase. With the same size and aspect ratio, the non-spherical particles had greater effect on the suspension viscosity than spherical particles. A correction factor was used to modify the viscosity model with the consideration of particle size, shape and aspect ratio. The prediction results of new modified viscosity model of the suspension finally showed good agreement with the measured experimental data.

1. Introduction

Entrained flow gasification technology was received widely application in the field of energy conversion. It allows for various combinations of electricity, liquid fuels, hydrogen, chemicals and heat with the characters of high efficiency and fuel flexibility [1]. Entrained flow gasifier usually operates at a high temperature (above the ash flow temperature) to ensure a good slagging condition for the stable operation [2,3]. The slag viscosity is the key factor in determining whether the slagging condition is stable and smooth.

The measurement of the viscosity of molten slag is significant not only for the theoretical research on melt, but also for the industrial application. Slag type with suitable fluidity at the low operation temperature for saving energy consumption is required to study [4]. The viscosity of slag with low melting point should be investigated to develop an improved gasification operation at low temperature. Molten slag is a solid-liquid two-phase mixture and solid particles do exist in slag in gasification processes. The viscosity of fully liquid slag increased with decreasing temperature, and the temperature dependence of the viscosity was usually expressed in the form of the Arrhenius relationship. With the precipitation of crystals from molten slag below the melting point, the slag behaved as a non-Newtonian fluid and the viscosity showed a sharp increase near the melting point [5]. Therefore, the characteristics of crystal precipitation during the cooling process of the molten slag were studied.

Xuan et al. [6–9] studied the influences of CaO, Fe_2O_3, SiO_2/Al_2O_3 on crystallization characteristics of synthetic coal slags. With the increase of CaO, crystallization of the slags became obvious, especially in which with a calcium content range between 15% and 35%. With a higher ratio of Fe_2O_3, more crystallization heat was released and the crystallization shifted to a higher temperature, potentially leading to a higher T_{cv} (Critical viscosity temperature) in viscosity. The kinetics under isothermal 1100 °C show that the growth rate of crystals increases with the addition of iron oxide. As the S/A ratio increased between the range of 1.5–3.5, the crystal was clear and energy barrier was significantly lowered and the crystallization ratio increased. Shen et al. [10] studied the effect of cooling process on the generation and growth of crystals in coal slag. Low cooling rate was beneficial to the generation of the crystals and long residence time below the initial crystallization temperature promoted the generation and growth of crystal. The influence of internal and external factors on slag viscosity was studied by Kong et al. [11–13]. They found that viscosities of glassy and

* Corresponding author at: Key Laboratory of Coal Gasification and Energy Chemical Engineering of Ministry of Education, East China University of Science and Technology, P.O. Box 272, Shanghai 200237, PR China.
E-mail address: hfliu@ecust.edu.cn (H. Liu).

https://doi.org/10.1016/j.fuel.2018.01.058
Received 9 September 2017; Received in revised form 30 November 2017; Accepted 16 January 2018

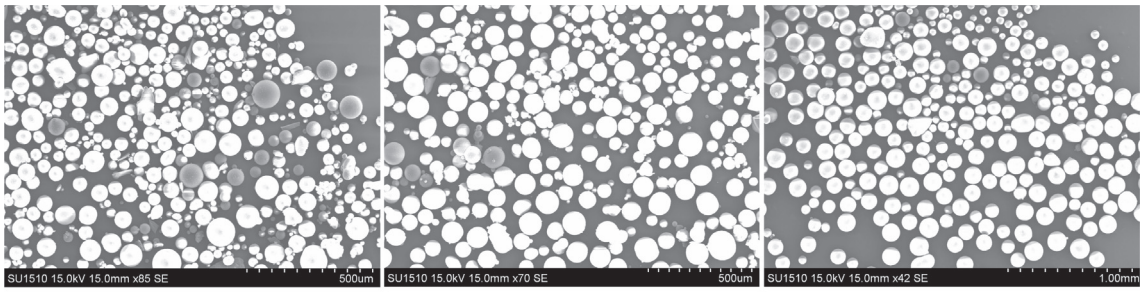

(a) D_a =68 μm (b) D_a =83 μm (c) D_a =100 μm

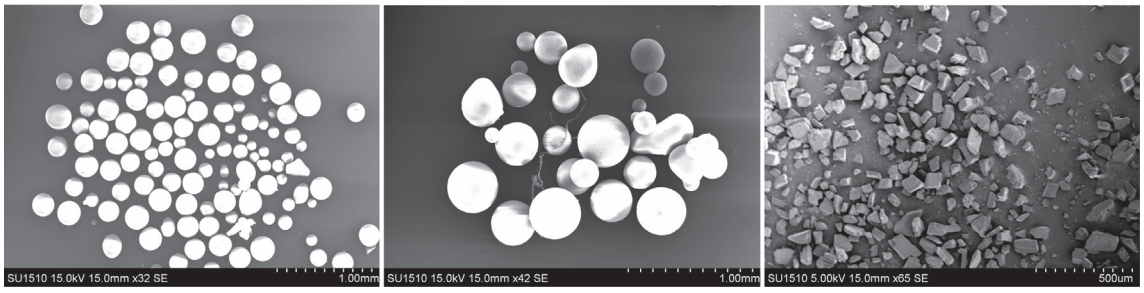

(d) D_a =187 μm (e) D_a =250 μm (f) D_a =187 μm

Fig. 1. The SEM images of particles with different sizes, (a)-(e) glass beads, (f) quartz sand particles.

crystalline slag both decreased with increasing cooling rate. The viscosity of the molten slag increased with the increasing the mass fraction of residual carbon. Kondratiev et al. [14] proposed chemical components such as P_2O_5, B_2O_3 possessed strong, highly covalent metal-oxygen bonds, leading to high liquid viscosities. Ilyushechkin et al. [15] concluded that slag viscosity depended on the slag bulk composition above the liquid temperature line. Zhang et al. [16] found that the viscosity of molten slag increased as increasing the volume fraction of TiC. Many researchers also proposed other factors (constant temperature, continuous cooling and different kinds of mineral) that affect the crystallization [17–21]. Owing to the difficulties in measurement, the viscosity of two-phase mixtures was hardly investigated. In view of the importance of slag viscosity in the optimization of gasification processes, researchers have used different models to estimate the viscosity of solid-liquid mixtures.

Early in the twentieth century, Einstein derived a linear equation about suspension viscosity based on Stokes equation [22,23]. Experiments were carried out to examine the applicability of Einstein's equation. The results demonstrated that this model could be only applied to dilute suspension [22]. For this reason, Simha used cell method to estimate the viscosity of liquid containing solid particles [24]. Following this approach, Happel [25], Zholkovskiy et al. [26], Sengun et al. [27], Malomuzh et al. [28], and Sherwood [29] had proposed modified models. Since the above models were derived from different boundary conditions, the prediction results were quite different at high particle volume fraction.

A number of semi-empirical models have been developed based on experiment data [30–33]. Jung et al. [34] proposed a comprehensive viscosity model for micro magnetic particles dispersed in silicone oil. The viscosity increased with the solid phase volume fraction. The magnetic field decreased with the shear rate and the temperature. The effect of temperature and solid phase volume fraction was well described by the Arrhenius model and the Krieger and Dougherty model [34]. The multiplied form of magneto rheological model was verified by the experiment data, and it was very useful for the prediction of shear viscosity under various operating conditions. Thionnet et al. [35] put forward the influence of the volume fraction, size and surface coating of hard spheres on the microstructure and rheological properties of model in mozzarella cheese. However, most of the experiment data had been generated using aqueous solutions. The big difference in viscosity between slag (usually > 0.1 Pa.s) and aqueous solution made the application of any of these models to slag system uncertain.

Koudratiev et al. [36] calculated the fractions of solid phase using F.A.C.T for some reported slags [37] and applied Roscoe model [31] to the two phase mixtures. The modified parameters for Roscoe equation with better accuracy and applicability were also reported. Wright et al. [38] measured the slag viscosity with either Al_2O_3, MgO or Fe_3O_4 particles. Great dependence of viscosity on rotation speed was reported when the fraction of particles was above 0.04.

A number of literatures studied the relationship between the suspension viscosity and the solid phase volume fraction, and obtained a series of models. However, most of the models assumed that the particles were spherical and nearly spherical, which was serious different from the actual situation. The aim of the research was to get a more accurate prediction model of the suspension viscosity. In this paper, the malt syrup and the particles with different size and morphology were chosen as the simulation medium to study. The effects of particle size, shape and aspect ratio of solid particles on the suspension viscosity were considered. Finally, a modified prediction model of slag viscosity were proposed and compared with the experimental data.

2. Experiment

2.1. Experiment material

The solvent used in the experiment was the syrup with a concentration of 70%. The density of the syrup was 1.28 g/cm^3 at 25 °C. The solid particles added to the syrup were glass beads (SiO_2 > 90%), wollastonite powders ($Ca_3(Si_3O_9)$) and quartz sand particles (SiO_2 > 67%). The density of glass beads was 1.5 g/cm^3. The average diameter of glass beads were screened to 68, 83, 100, 187 and 250 μm respectively. The density of wollastonite particle was 1.3 g/cm^3 and its shape was acicular, the average particle size were screened to 12, 18.75 and 37.5 μm respectively. The aspect ratio of the wollastonite particles

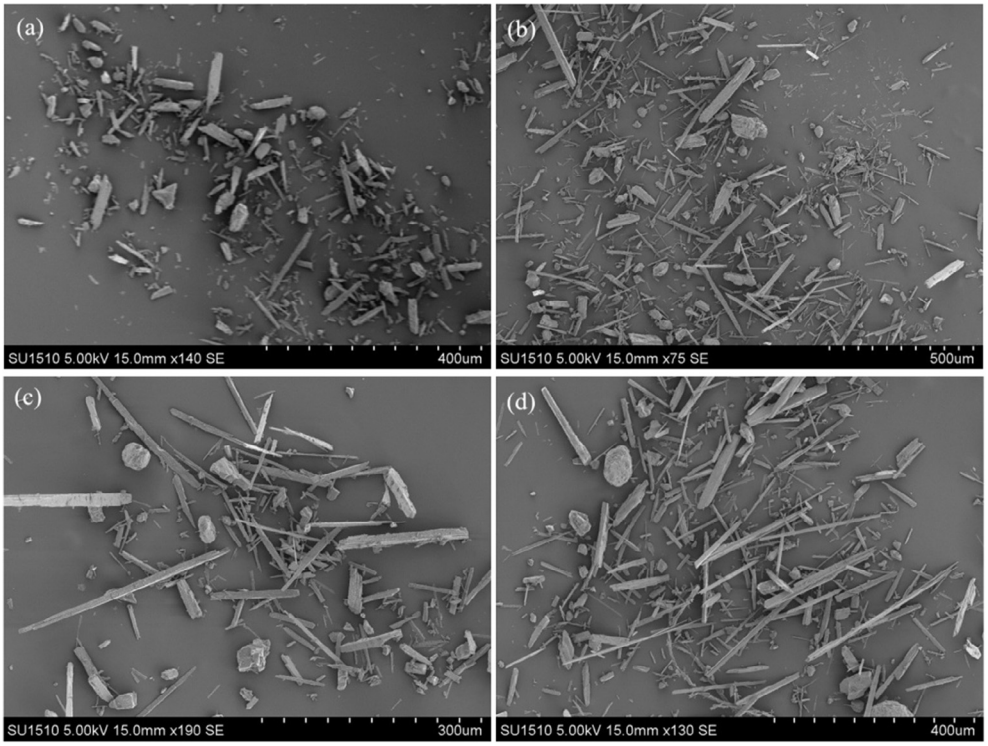

Fig. 2. The SEM images of wollastonite particles with different aspect ratios. (a) 5:1, (b) 10:1, (c) 15:1, (d) 20:1.

Table 1
The properties of the samples.

Material	Shape	Size/μm	Aspect ratio
Glass beads	Spherical	68	1
		83	1
		100	1
		187	1
		250	1
Quartz sand	Cube	187	1
Wollastonite	Acicular	12	10
		18.75	10
		37.5	10
		37.5	5
		37.5	15
		37.5	20

included 5: 1, 10: 1, 15: 1 and 20: 1 when the size was 37.5 μm. The density of quartz sand particles was 1.5 g/cm^3. Quartz sand particles were approximate cube whose average size was 187 μm. The SEM images of the samples are shown in Fig. 1 and Fig. 2. The properties of the samples are shown in Table 1, where d_a is the average size of the particle.

2.2. Experiment method

The shape and aspect ratio of the particle were observed by SV-1510 SEM (Hitachi Company, Japan). The size of particle was measured by Mastersizer 2000 (Malvern, UK). The suspension viscosity was measured by a Bohlin CVO rheometer (Malvern, UK) at 25 ± 0.1 °C. The rheometer is consisted of a cup centered on a turntable with a rotor concentrically suspended within it. The diameter of rotor and cylinder was 25 and 37 mm respectively. The height of rotor and cylinder was 43.5 and 45 mm respectively. The standard silicone oil was used to calibrate the viscosity and the experimental error was controlled within 1%. The syrup was placed in the annular space between the inner rotor and outer cylinder for measurement and the particles were added with the volume fraction of 10%, 20%, 30%, 40% and 50% respectively. The suspension viscosity was measured by logarithmically increasing the shear rate from 0.01 s^{-1} to 100 s^{-1} over a period of 100 s, then keep this rate for 50 s. After that, the rate was decreased to 0.01 s^{-1} within 100 s. The viscosity value at a shear rate of 100 s^{-1} was used as the apparent viscosity of the suspension. The yield stress is defined as the stress at which the sample begins to deform plastically. Measurements were repeated three times to ensure that the results were reproducible.

3. Results and discussion

3.1. Effect of particle size on viscosity

3.1.1. Suspension viscosity of spherical particles

For spherical particles, the changes of the viscosity of suspension with different solid phase volume fraction and particle sizes are shown in Fig. 3(a). It can be seen from the Fig. 3(a) that the suspension viscosity increased with the increase of the volume fraction under the same particle size, and the increase of viscosity was more obvious when the volume fraction reached 30% or more. When the volume fraction was 10%, the relative viscosity was about 1.2, and when the volume fraction was 50%, the relative viscosity of the suspension with particle size of 68 μm was 4.17, which increased 2.48 times. However, the relative viscosity of suspension with particle size of 250 μm was 2.29, which only increased 0.9 times. This phenomenon could be explained by the fact that the increase in the volume fraction of solid particles resulting in the enhance of solid interaction in the unit volume to the same particle size. The viscous resistance of the fluid flowability raised with the fluid strength increasing, which resulted the increase of suspension viscosity. With the same solid phase volume fraction, the suspension viscosity decreased with the increase of particle size, and the change of suspension viscosity was more obvious when the volume fraction was more than 30%. When the solid phase volume fraction reached to 50%, the relative viscosity increased by about 0.91 times when the particle size was increased by 2 times. This indicated that the particle size had a large effect on the suspension viscosity under high solid phase volume

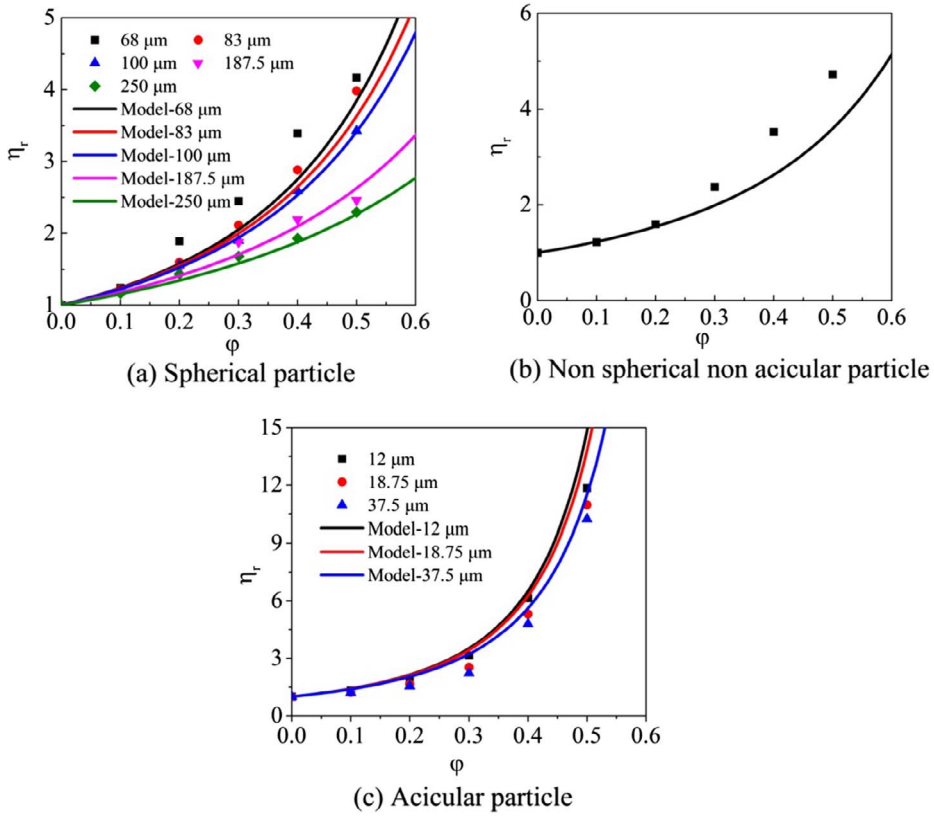

Fig. 3. Viscosity curves of the suspension with different particles.

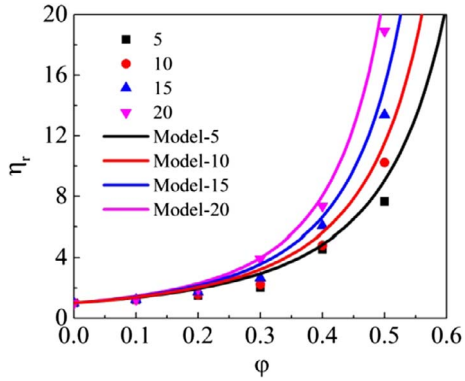

Fig. 4. Viscosity curves of the suspension with different aspect ratio particles.

fraction. The reason was that the interaction of particles in unit volume was weakened with the increase of particle size, hence decreasing the suspension viscosity. With the decrease of the solid phase volume fraction, the probability of interaction between the particles was much smaller, thus the variation of the suspension viscosity was more obvious under the high solid phase volume fraction.

3.1.2. Suspension viscosity of non-spherical non-acicular particles

For the non-spherical non-acicular particles, changes of the suspension viscosity with different solid phase volume fractions are shown in Fig. 3(b). It can be seen from the Fig. 3(b), with the increase of the solid phase volume fraction, the suspension viscosity also increased. The result was consistent with the conclusion of spherical particles. With the same particle size, the non-spherical particle had more influence on the suspension viscosity than the spherical particle.

3.1.3. Suspension viscosity of acicular particles

For the acicular particles, changes of the suspension viscosity with different solid phase volume fraction are shown in Fig. 3(c). As can be seen from Fig. 3(c), the suspension viscosity increased obviously with the increase of the solid phase volume fraction. When the volume fraction was 10%, the relative viscosity was about 1.31, and when the volume fraction reached to 50%, the relative viscosity increased to about 11.84, rising about 8 times. This indicated that the effect of acicular particles was much greater than that of spherical particles under the same solid phase volume fraction. This phenomenon was particularly obvious at high solid phase volume fraction. While under the same solid phase volume fraction, the impact of the particle size on the suspension viscosity was smaller. When the volume fraction was 50%, the particle size increased by 2 times, the value of relative viscosity increased only by 0.16 times.

3.2. Effect of aspect ratio on viscosity

The curves drawn from the experiment data are shown in Fig. 4. It can be seen from the Fig. 4 that as the solid phase volume fraction increased, the suspension viscosity increased rapidly. When the solid phase volume fraction was 10%, the relative viscosity of the suspension was 1.22. When the solid phase volume fraction reached 50% and the particle aspect ratio was 5, the relative viscosity of the suspension was 7.65, which increased by 5.27 times. However, with the aspect ratio of 20, the relative viscosity of the suspension was 18.91, with an increase of 14.5 times. With the increase of the aspect ratio, the suspension viscosity increased under the same solid phase volume fraction, and the performance was more obvious under the high volume fraction. When the solid phase volume fraction was 50%, the relative viscosity of the suspension increased by 1.47 times. This indicated that the effect of the aspect ratio of the particles on the suspension viscosity was significant. The result was mainly due to that with the increase in the solid phase volume fraction, the interaction between the solid phases also increased, resulting in the increase of suspension viscosity. Furthermore, under the high volume fraction, the greater the aspect ratio, the greater

increase of the suspension viscosity with more frequent interaction.

3.3. Model comparison

Einstein model [22] was widely used among the prediction models for the suspension viscosity. For low viscosity fluid with hard ball particles, Einstein assumed that the radius of the hard sphere particles was much smaller than the radius of the measuring device and much larger than the molecular radius of the solvent. At the same time, no interaction between the hard sphere particles was appeared, and the hard sphere particles were in the laminar flow. In this case, the relationship between the volume fraction of the particles and the viscosity of the fluids containing the particles was given:

$$\eta_r = 1 + \alpha\varphi, \tag{1}$$

where η_r is the relative viscosity, α is a constant value, which is related to the shape and variability of the particles. In the Einstein model [22], the particles are hard spherical and α is 2.5.

However, the Einstein model did not consider the interaction between particles, it can only be applied to low viscosity fluids. On the basis of Einstein model, Roscoe gave the equation in the whole concentration range [31]:

$$\eta_r = (1-\beta\varphi)^{-2.5}. \tag{2}$$

where β is the correction factor. When the spherical particle size varies, the value of β is 1. When the volume fraction of spherical particles with the same size is larger, β is 1.35.

The equations of different models are shown in Table 2. The comparison of the viscosity between classic models and experiment data is shown in Fig. 5. It can be seen from Fig. 5, viscosity predicted by the classical models differed greatly with the actual viscosity, especially when the solid phase volume fraction reached above 30%, and the gap was more obvious. With different particles, these models could not made accurate predictions. These models only considered the effect of solid phase volume fraction on suspension viscosity, while ignoring other factors (particle size, particle shape, particle aspect ratio). Thus limitations in the prediction of the suspension viscosity of the classical models were existed. Results showed that it was necessary to build a model which considered the effect of three factors on the suspension viscosity. The prediction of the suspension viscosity must have better applicability with suspension containing different particles. According to the comparison, Einstein-Roscoe model was used in this study because of its better agreement with the experiment data.

3.4. Model modification

Roscoe assumed the particle content as the main influencing factor in the Eq. (2), without considering the effect of the particle shape. In Eq. (1), α represented the effect of particle deformability and shape on the viscosity of the particulate fluid. Therefore, this study focused on the impact of particle morphology on the suspension viscosity. The factor (β) was introduced into the Einstein-Roscoe model in order to improve the accuracy.

From the above analysis, it can be seen that the particle size, particle shape and particle aspect ratio had a certain impact on the suspension viscosity. For the same particle shape and aspect ratio, the viscosity of the suspension with the same volume fraction of particles increased with the decrease of the particle diameter. For the same particle size and aspect ratio, the effect of the non-spherical particles on the suspension viscosity was larger than spherical particles. For the same particle size and shape of the particles, the greater the aspect ratio, the greater changes in the suspension viscosity. Therefore, it was necessary to study the comprehensive impacts of the three factors on the suspension viscosity. The experiment data were used to modify Eq. (2), and the correction factor was expressed as:

$$\beta = \beta_1\beta_2\beta_3, \tag{3}$$

where β_1, β_2 and β_3 were the correction parameters respecting to particle size, shape and aspect ratio respectively. In addition, considering the aspect ratio of 1, the difference between the spherical particles and the cube particles showed that the particle shape had greater impacts on the suspension viscosity. The spherical degree was introduced. According to the literature, the spherical degree of cube was 0.81 [40].

From the Figs. 6 and 7, it can be seen that the relationship between the correction factor β and the influencing factors was exponential with the semi-logarithmic coordinates. With the increase of the particle size, the value of β decreased. The minimum value reached 0.55. Under the same particle size, minor difference in the value of β of the different solid phase volume fractions was within acceptable limitations. With the increase of the particle aspect ratio, the value of β also increased, and the maximum value reached to 1.38. Considering the different influencing factors separately, the basic form of equations between β and the influencing factors are given in Table 3.

Through the fitting of the experiment data and the use of Eq. (3), β can be expressed as:

$$\beta = 0.9672Ce^{-0.0022d}e^{0.0126(\theta-1)}, \tag{4}$$

where β was the correction factor, d was the particle size, θ was the particle aspect ratio. C was constant, which was related to the particle

Table 2
Equations of different models.

Model	Equation
Einstein	$\eta_r = 1 + 2.5\varphi$ [22]
Einstein-Roscoe	$\eta_r = (1-\varphi)^{-2.5}$ [31]
Batchelor	$\eta_r = 1 + 2.5\varphi + 6.5\varphi^2$ [39]
Vand-Roscoe	$\eta_r = (1-1.35\varphi)^{-2.5}$ [31]

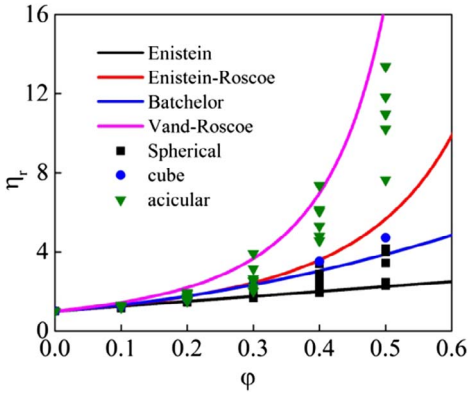

Fig. 5. The comparison of the viscosity between classic models and experiment data.

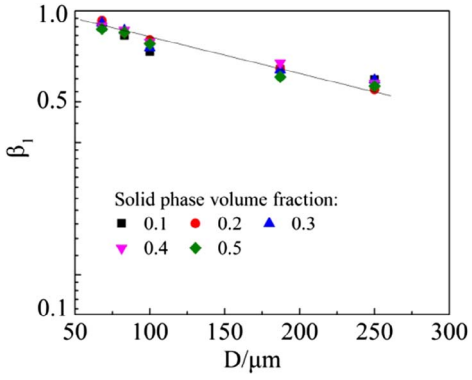

Fig. 6. The relationship between β_1 and the different size of glass beads particles.

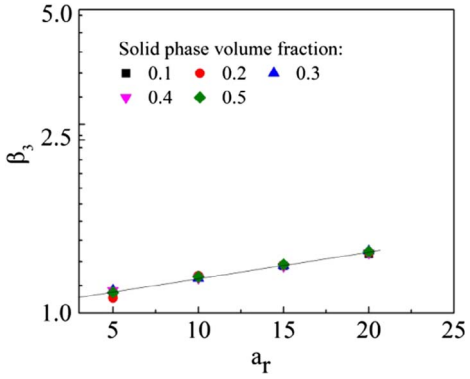

Fig. 7. The relationship between β_3 and different aspect ratio of acicular particles.

Table 3
The relationships between β and different influencing factors.

Factor	β
Size	$\beta_1 = A_1 e^{B_1 d}$.
Shape	$\beta_2 = C$
Aspect ratio	$\beta_3 = A_3 e^{B_3 a_r}$

*Where d was the particle size, a_r was the particle aspect ratio. A_1, B_1, A_3, B_3 and C were constants.

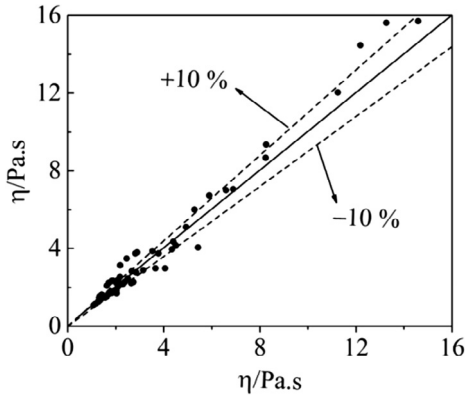

Fig. 8. The comparison of the suspension viscosity between the model and experiment data. The dashed lines represented ± 10% error bars. The cross axis denoted the suspension viscosity obtained by experiment. The vertical axis denoted the suspension viscosity obtained by the model.

shape, when the particles were spherical, C was 1, when the particles were non-spherical, C was 1.235.

The viscosity of the suspension with different solid phase volume fraction was predicted by the Eq. (2). The comparison of the prediction results and the actual values are shown in Fig. 8. The cross axis indicated the suspension viscosity obtained by experiment. The vertical axis indicated the suspension viscosity obtained by the model. It can be seen from the Fig. 8 that the values calculated by model and experiment results agreed well the average relative error of 4.3%. However, According to calculation, the average relative error of Einstein, Einstein-Roscoe, Batchelor and Vand-Roscoe were −123.8%, 34.9%, −79.5% and 83.9% respectively.

4. Conclusion

In this paper, the factors that affect the suspension viscosity were mainly studied, including the particle size, shape and aspect ratio of the solid particles. The Einstein-Roscoe equation was modified on the basis of a series of experimental data, and the model of the suspension viscosity respecting to the solid phase volume fraction was obtained. The conclusions are as follows:

(1) The suspension viscosity increased with the decrease of the particle size under the same volume fraction of particles, and the suspension viscosity increased more obviously under the high solid phase volume fraction.
(2) Particle shape also had effects on the suspension viscosity, and the effect of the non-spherical particles on the suspension viscosity was larger than that of the spherical particles
(3) The suspension viscosity increased with the increase of the particle aspect ratio, and the larger the aspect ratio, the more the suspension viscosity increased.
(4) Based on the influence of three factors, the equation of suspension viscosity respecting to the solid phase volume fraction was obtained, and the prediction results of the suspension viscosity agreed with the experiment data. However, this paper simplify the influence of maximum packing fraction and shear rate on the suspension viscosity which would be studied in future work.

Acknowledgments

This study was supported by the National Natural Science Foundation of China (U1402272), the Foundation of Shanghai Science and Technology Committee (14dz1200100), the National Nature Science Foundation of China (21376082), and the Foundation of State Key Laboratory of Coal Conversion (Grant No. J16-17-301).

References

[1] Yamashita K, Barreto L. Energyplexes for the 21st century: coal gasification for co-producing hydrogen, electricity and liquid fuels. Energy 2005;30:2453–73.
[2] Krishnamoorthy V, Pisupati S. A critical review of mineral matter related issues during gasification of coal in fixed, fluidized, and entrained flow gasifiers. Energies 2015;8:10430–63.
[3] Gong X, Lu WX, Guo XL, Dai ZH, Liang QF, Liu HF, et al. Pilot-scale comparison investigation of different entrained-flow gasification technologies and prediction on industrial-scale gasification performance. Fuel 2014;129:37–44.
[4] Jang D, Kim Y, Shin M, Lee J. Kinetics of carbon dissolution of coke in molten iron. Metall Mater Trans B 2012;43:1308–14.
[5] Seftharaman S, Sichen D, Sridhar S, Mills KC. Estimation of liquidus temperatures for multicomponent silicates from activation energies for viscous flow. Metall Mater Trans B 2000;31:111–9.
[6] Xuan WW, Whitty KJ, Guan QL, Bi DP, Zhan ZH, Zhang JS. Influence of CaO on crystallization characteristics of synthetic coal slags. Energy Fuels 2014;28:6627–34.
[7] Xuan WW, Whitty KJ, Guan QL, Bi DP, Zhan ZH, Zhang JS. Influence of Fe_2O_3 and atmosphere on crystallization characteristics of synthetic coal slags. Energy Fuels 2015;29:405–12.
[8] Xuan WW, Whitty KJ, Guan QL, Bi DP, Zhan ZH, Zhang JS. Influence of SiO_2/Al_2O_3 on crystallization characteristics of synthetic coal slags. Fuel 2015;144:103–10.
[9] Xuan WW, Zhang JS, Xia DH. Crystallization characteristics of a coal slag and influence of crystals on the sharp increase of viscosity. Fuel 2016;176:102–9.
[10] Shen ZJ, Li RX, Liang QF, Xu JL, Liu HF. Effect of cooling process on the generation and growth of crystals in coal slag. Energy Fuels 2016;30:5167–73.
[11] Kong LX, Bai J, Li W, Wen XD, Li XM, Bai ZQ, et al. The internal and external factor on coal ash slag viscosity at high temperatures, Part 1: effect of cooling rate on slag viscosity, measured continuously. Fuel 2015;158:968–75.
[12] Kong LX, Bai J, Li W, Wen XD, Liu XC, Li XM, et al. The internal and external factor on coal ash slag viscosity at high temperatures, Part 2: effect of residual carbon on slag viscosity. Fuel 2015;158:976–82.
[13] Kong LX, Bai J, Li W, Wen XD, Li XM, Bai ZQ, et al. The internal and external factor on coal ash slag viscosity at high temperatures, Part 3: effect of CaO on the pattern of viscosity–temperature curves of slag. Fuel 2016;179:10–6.
[14] Kondratiev A, Jak E. Predicting coal ash slag flow characteristics (viscosity model for the Al_2O_3–CaO–'FeO'–SiO_2 system). Fuel 2001;80:1989–2000.
[15] Ilyushechkin AY, Hla SS, Roberts DG, Kinaev NN. The effect of solids and phase compositions on viscosity behaviour and T_{CV} of slags from Australian bituminous coals. J Non-Cryst Solids 2011;357:893–902.
[16] Zhang GH, Zhen YL, Chou KC. Influence of TiC on the viscosity of CaO–MgO–Al_2O_3–SiO_2–TiC suspension system. ISIJ Int 2015;55:922–7.
[17] Xu J, Zhao F, Guo QH, Yu GS, Liu X, Wang FC. Characterization of the melting behavior of high-temperature and low-temperature ashes. Fuel Process Technol 2015;134:441–8.
[18] Gan L, Zhang CX, Zhou JC, Shangguan FQ. Continuous cooling crystallization kinetics of a molten blast furnace slag. J Non-Cryst Solids 2012;358:20–4.

[19] Shen ZJ, Liang QF, Zhang BB, Xu JL, Liu HF. Effect of continuous cooling on the crystallization process and crystal compositions of iron-rich coal slag. Energy Fuels 2015;29:3640–8.
[20] Trasi NS, Baird JA, Kestur US, Taylor LS. Factors influencing crystal growth rates from undercooled liquids of pharmaceutical compounds. J Phys Chem B 2014;118:9974–82.
[21] Burkhard DJM. Nucleation and growth rates of pyroxene, plagioclase, and Fe-Ti oxides in basalt under atmospheric conditions. Eur J Mineral 2005;17:675–86.
[22] Einstein A. A new determination of molecular dimensions. Ann Phys 1906;19:289–306.
[23] Einstein A. Berichtigung zu meiner Arbeit:"Eine neue Bestimmung der Moleküldimensionen". Ann Phys 1911;339:591–2.
[24] Simha R. A treatment of the viscosity of concentrated suspensions. J Appl Phys 1952;23:1020–4.
[25] Happel J. Viscosity of suspensions of uniform spheres. J Appl Phys 1957;28:1288–92.
[26] Zholkovskiy EK, Adeyinka OB, Masliyah JH. Spherical cell approach for the effective viscosity of suspensions. J Phys Chem B 2006;110:19726–34.
[27] Sengun M, Probstein R. Bimodal model of suspension viscoelasticity. J Rheol 1997;41:811–9.
[28] Malomuzh N, Orlov E. A new version of the cell method of determining the suspension viscosity. Colloid J 2002;64:725–33.
[29] Sherwood J. Cell models for suspension viscosity. Chem Eng Sci 2006;61:6727–31.
[30] Mooney M. The viscosity of a concentrated suspension of spherical particles. J Colloid Sci 1951;6:162–70.
[31] Roscoe R. The viscosity of suspensions of rigid spheres. Br J Appl Phys 1952;3:267.
[32] Batchelor GK, Green JT. The determination of the bulk stress in a suspension of spherical particles to order c2. J Fluid Mech 1972;56:401–27.
[33] Thomas DG. Transport characteristics of suspension: VIII. A note on the viscosity of Newtonian suspensions of uniform spherical particles. J Colloid Sci 1965;20:267–77.
[34] Jung ID, Kim M, Park SJ. A comprehensive viscosity model for micro magnetic particle dispersed in silicone oil. J Magn Magn Mater 2016;404:40–4.
[35] Thionnet O, Havea P, Gillies G, Lad M, Golding M. Influence of the volume fraction, size and surface coating of hard spheres on the microstructure and rheological properties of model mozzarella cheese. Food Biophys 2016;12:33–44.
[36] Kondratiev A, Jak E. Modeling of viscosities of the partly crystallized slags in the Al_2O_3-CaO-"FeO"-SiO_2 system. Metall Mater Trans B 2001;32:1027–32.
[37] Oh MS, Brooker DD, De Paz EF, Brady JJ, Decker TR. Effect of crystalline phase formation on coal slag viscosity. Fuel Process Technol 1995;44:191–9.
[38] Wright S, Zhang L, Sun SY, Jahanshahi S. Viscosities of calcium ferrite slags and calcium alumino-silicate slags containing spinel particles. J Non-Cryst Solids 2001;282:15–23.
[39] Batchelor GK. Sedimentation in a dilute polydisperse system of interacting spheres. 1. general-theory. J Fluid Mech 1982;119:379–408.
[40] Liu MF, Chen SF, Liu YY. Characterization of sphericity and wall thickness uniformity of thick-walled hollow microspheres. High power laser and particle beams 2014;26(2):0220171–220175.